Aalborg Universitet

Sizing of Hybrid Supercapacitors and Lithium-Ion Batteries for Green Hydrogen Production from PV in the Australian Climate

Ibrahim, Tarek; Kerekes, Tamas; Sera, Dezso; Mohammadshahi, Shahrzad S.; Stroe, Daniel-Ioan

Link to publication from Aalborg University

Article

Sizing of Hybrid Supercapacitors and Lithium-Ion Batteries for Green Hydrogen Production from PV in the Australian Climate

Tarek Ibrahim [1], Tamas Kerekes [1,*], Dezso Sera [2], Shahrzad S. Mohammadshahi [2] and Daniel-Ioan Stroe [1]

[1] Department of Energy, Aalborg University, 9220 Aalborg, Denmark
[2] School of Electrical Engineering & Robotics, Queensland University of Technology, Brisbane 4000, Australia
[*] Correspondence: tak@energy.aau.dk

Abstract: Instead of storing the energy produced by photovoltaic panels in batteries for later use to power electric loads, green hydrogen can also be produced and used in transportation, heating, and as a natural gas alternative. Green hydrogen is produced in a process called electrolysis. Generally, the electrolyser can generate hydrogen from a fluctuating power supply such as renewables. However, due to the startup time of the electrolyser and electrolyser degradation accelerated by multiple shutdowns, an idle mode is required. When in idle mode, the electrolyser uses 10% of the rated electrolyser load. An energy management system (EMS) shall be applied, where a storage technology such as a lithium-ion capacitor or lithium-ion battery is used. This paper uses a state-machine EMS of PV microgrid for green hydrogen production and energy storage to manage the hydrogen production during the morning from solar power and in the night using the stored energy in the energy storage, which is sized for different scenarios using a lithium-ion capacitor and lithium-ion battery. The mission profile and life expectancy of the lithium-ion capacitor and lithium-ion battery are evaluated considering the system's local irradiance and temperature conditions in the Australian climate. A tradeoff between storage size and cutoffs of hydrogen production as variables of the cost function is evaluated for different scenarios. The lithium-ion capacitor and lithium-ion battery are compared for each tested scenario for an optimum lifetime. It was found that a lithium-ion battery on average is 140% oversized compared to a lithium-ion capacitor, but a lithium-ion capacitor has a smaller remaining capacity of 80.2% after ten years of operation due to its higher calendar aging, while LiB has 86%. It was also noticed that LiB is more affected by cycling aging while LiC is affected by calendar aging. However, the average internal resistance after 10 years for the lithium-ion capacitor is 264% of the initial internal resistance, while for lithium-ion battery is 346%, making lithium-ion capacitor a better candidate for energy storage if it is used for grid regulation, as it requires maintaining a lower internal resistance over the lifetime of the storage.

Keywords: green hydrogen; PV; supercapacitor; DC microgrids; lithium-ion batteries; sizing

1. Introduction

Energy can be stored in different forms, and one of these forms is fuel. Fuel was used since the industrial revolution in the 18th century to run the machines and used for thousands of years earlier in heating, lighting and cooking, which makes it a more conventional means of energy that humans use in their life. The main challenge of using fuel is its chemical irreversibility and burning releases compounds such as CO_2, which contributes to the greenhouse gas effect. One method to overcome the side effect of fuel is to use fuels that do not release CO_2 when consumed, such as hydrogen. The problem with using hydrogen as a fuel is that its industrial production comes mostly from fossil and nonrenewable sources. From that, the importance of green hydrogen becomes clear, and researchers are working on more efficient ways of producing hydrogen from renewable sources.

The fact that green hydrogen production only requires water and a renewable energy source, promoted the development of microgrids for green hydrogen production. Renewable microgrids have been widely used for providing power to homes in rural areas where the power grid is not available [1].

Pairing hydrogen production/storage with solar or wind microgrid batteries powers residential areas in a zero-emission manner.

One of the challenges of using solar power for hydrogen production is its intermittent and unpredictable power output. The hydrogen production cell is sensitive to power fluctuations where multiple shutdowns and restarts accelerate the degradation of the cell. Extending the life of the hydrogen cell happens by putting the cell in idle mode, where it becomes 10% of the production load.

Overcoming the power intermittency and securing the idle mode required power from PV is achieved by including energy storage in the microgrid. Currently, the most used storage technology integrated with solar and wind power systems is based on Lithium-ion (Li-ion) batteries [2]; nevertheless, due to the high cost, the need for stable temperature, and the limited lifetime of Li-ion batteries [3], there is a need for alternative electrical energy storage solutions to keep up with the development and integration of renewable plants. One such technology is represented by Li-ion capacitors (LiCs). LiCs are a promising solution for energy storage [4], which can overcome some of the disadvantages of Li-ion batteries, which were mentioned before.

Conventional systems for green hydrogen production are based on grid-connected facilities supplied by renewable sources and use the excess energy for hydrogen production as a method of storing the energy. The current focus in the field of green hydrogen production is on utilizing distributed microgrids or retrofitting existing renewable energy plants to optimize production [5]. Energy storage (ES) based on LiC is compared with LiB ES, with a focus on size, remaining capacity, and internal resistance, to determine the best fit for green hydrogen production. The energy management system (EMS) is being developed to ensure the efficient operation of the electrolyser and the ES production [5].

The ES sizing optimization problems are divided into two parts: system modeling with input parameters and real data from the system location, and output part for evaluating the outputs such as SoC [6]. A sizing algorithm is then used to iterate the simulation for different input parameters and search for the optimal solution according to the system criteria that shall be met. Searching methods can be used for sizing such systems, such as directed search [7] or the sparrow search algorithm, if required optimization is multidimensional [8].

There is increasing attention on establishing a DC microgrid to eliminate AC power conversions and further increase efficiency [9]. The goal is to maximize the production of green hydrogen and supply commercial needs through the main production of the microgrid or through excess energy instead of storing it in batteries.

The sizing of the storage needs to be optimized for outdoor climatic conditions at the grid's location (ES has no temperature-controlled environment). The capacity of Li-ion batteries and Li-ion capacitors is dependent on the temperature at the site location. The degradation rate of both storage technologies is also dependent on the temperature and number of full equivalent cycles (FEC) of the cell. Increasing the size will reduce the FEC of the storage and will increase its lifetime but will also increase its cost. Thus, an energy management system (EMS) shall be used to maximize the hydrogen production and the expected life of storage cells and secure the power of the load in idle mode. This work aims to propose and provide an analysis of two storage technologies and compare them to suggest the best technology for green hydrogen production applications.

This paper is divided into the following sections: Section 2, Green hydrogen production system; Section 3, Li-ion capacitor and Li-ion battery degradation behavior; Section 4, Sizing results for the Li-ion capacitor and Li-ion battery; Section 5, Sensitivity analysis of Li-ion capacitor and Li-ion battery; Section 6, Discussion and future work Section 7, and Conclusion.

2. Green Hydrogen Production System

In this paper, the main focus is to optimize the ES size that assists hydrogen production from PV power. This section gives an insight into the components and operation of the system.

The green hydrogen production from a PV facility consists of PV arrays, an energy storage system, and a hydrogen generator through electrolysis (Electrolyser).

There are different water electrolysis technologies such as Alkaline Electrolysis Cells, Proton Exchange Membrane (PEM), and Solid Oxide Electrolysis Cells. PEM electrolysis technology is widely established as an efficient and suitable option for hydrogen production from renewable-powered systems due to its high efficiency, and ability to produce high-purity hydrogen [10,11]. PEM has some challenges, such as the use of expensive catalyst materials and shorter-life membrane materials. To maintain a long lifetime of the electrolyser, an EMS is required.

Replicating the system model of the solar hydrogen pilot plant in greater Brisbane [5], the electrolyser power is 66% of the PV nominal power. The aim of this work is to demonstrate the DC off-grid hydrogen production as shown in Figure 1. The figure presents the DC Microgrid for green hydrogen production used [9,12], as DC microgrids produce hydrogen more efficiently by eliminating unnecessary AC power conversions from the system. In [9] as in Figure 1, the power conversion between a 380V DC bus supplied by PV powers the electrolyser, while a 48V bus is tied to the ES, and the 380 V–48 V is powered through a bidirectional DC-DC converter. The power electronics of the system are not considered in this work, but the storage and EMS components of the system are the focus. The modeled system in this work consists of a nominal 1500 W PV and 1000 W PEM electrolyser, an ES that uses LiC or LiB cells, and an EMS that governs the operation of the electrolyser and the power flow from/to the ES.
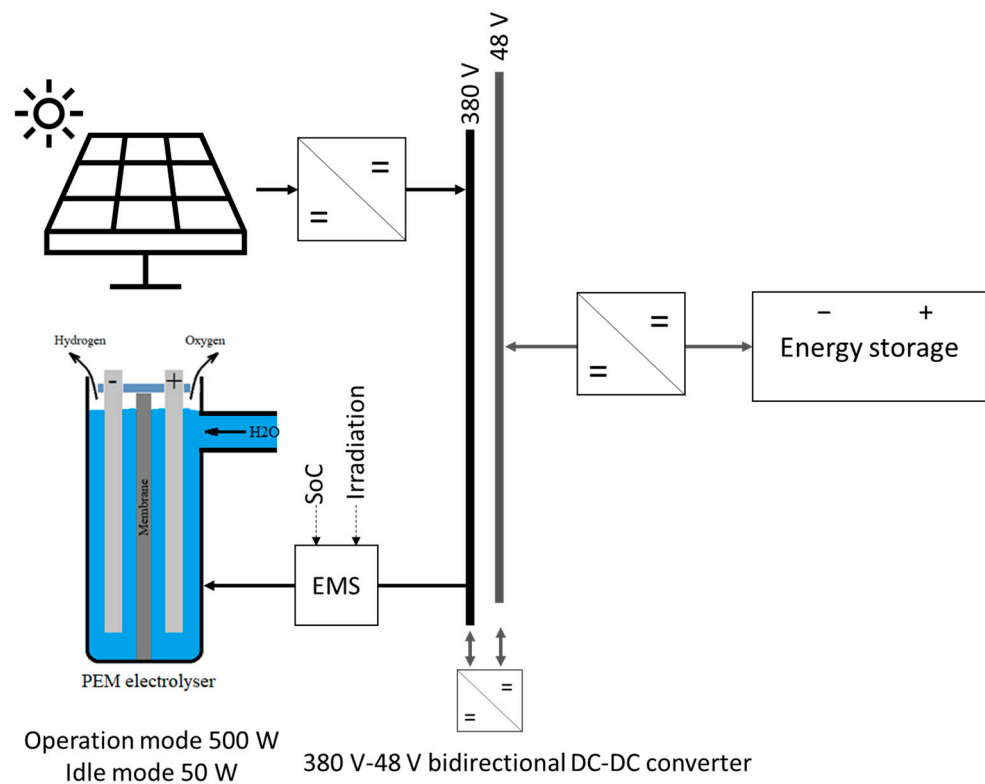

Figure 1. The considered microgrid for green hydrogen production.

In Figure 2, The PEM electrolyser has three stats of operations managed by the EMS as follows [13]:

- H2 Production mode: During this state, the electrolyser is producing hydrogen at its rated production capacity powered by the PV panels generation; if the PV generation drops during the day, the ES will substitute.
- Standby/Idle mode: During this state, the electrolyser consumes 10% of its rated production capacity power to sustain the required temperature and pressure of the electrolyser. The electrolyser is ready to return to the production state in a short mode transitioning time.
- Off/Failure mode: During this state, the electrolyser is in a total shutdown, where it losses the pressure and the temperature required by the electrolyser.
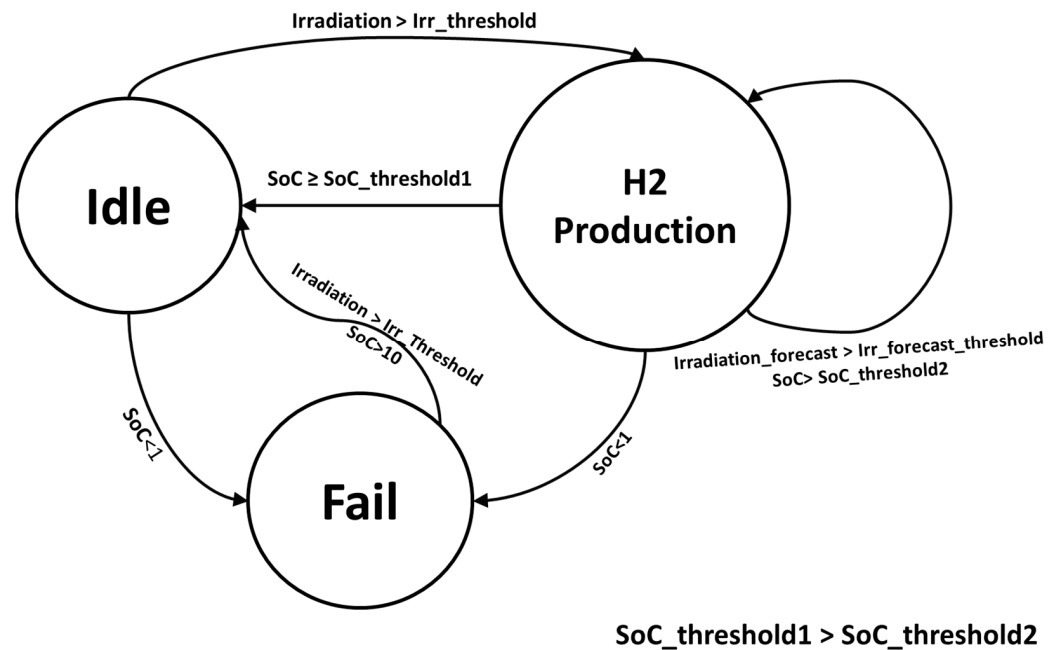

Figure 2. EMS state machine for the electrolyser.

There are data inputs that govern the electrolyser load transitions from one state to the other such as the state of charge (SoC) of the ES, solar irradiation, and solar irradiation forecast. The irradiation is the current solar irradiation, and the irradiation forecast is the irradiation predicted for the next day. Transitions from each state to the other are as follows:

- The transition from idle to production mode takes place when the solar irradiation is higher than a specific threshold (Irr_threshold). This is considered a hot start of the electrolyser because it sustains its required startup pressure and temperature.
- The transition from production to idle mode takes place when the SoC of the ES drops to a certain threshold where the remaining stored energy in the ES will power the electrolyser with 10% of its rated power to avoid the total shutdown situation. The electrolyser remains in the production mode even after crossing the ES SoC threshold if the Irradiation forcast the next day is enough to generate energy that will sustains the system for the next 24 h.
- A transition to the fail mode where a total shutdown and depressurization of the electrolyser occurs when the ES is fully discharged and SoC is almost zero. Transitioning from the fail mode to the idle mode is considered a cold start where the temperature increases and pressure builds up to be in the idle state conditions, which takes more time than the hot start.

Irradiation forecast signal selects whether the transition from production to idle mode happens at a high SoC (SoC_threshold1) and the night production is reduced or at a low SoC (SoC_threshold2) where the night production is increased.

3. Li-ion Capacitor and Li-ion Battery Degradation Behavior

3.1. Li-ion Capacitor and Li-ion Battery under Consideration

Hybrid supercapacitors, also known as lithium-ion capacitors (LiC), are an emerging technology that combines the advantages of an electric double-layer capacitor (EDLC) with those of a lithium-ion battery. LiC has a high-power density and can withstand temperature fluctuations, making it suitable for outdoor applications. It also has a longer cycle lifetime and higher power density than lithium-ion batteries (LiB). LiB, on the other hand, is more susceptible to degradation due to temperature fluctuations and has a lower power density. Additionally, LiB is more sensitive to fluctuations in power supply and requires a higher oversizing to prevent degradation.

In outdoor applications where ES is not placed in a temperature-controlled environment, LiC offers several advantages over LiB as an energy storage solution. Its ability to withstand temperature fluctuations and its longer cycle lifetime make it a more reliable option. Additionally, having an optimized size for the ES reduces the overall cost of the system. A comparison of the degradation behavior between LiB and LiC showed that LiC had better performance in terms of cycle life compared to LiB but the bottleneck is in the calendar life of the LiC [14]. In Table 1 the specifications of the used LiB and LiC in this study are presented.

Table 1. Datasheet parameters of LiB and LiC.

Property	LiC	LiB
Nominal capacity	4 Ah	13 Ah
Nominal voltage	3.2 V	2.26 V
Maximum voltage	4 V	2.9 V
Minimum voltage	2.5 V	1.5 V
Max. charge/discharge current	30 A	130 A
Calendar life	5 years	25 years
Internal resistance	6 mΩ	1.5 mΩ
Specific energy	48.8 Wh/kg	74 Wh/kg
Energy density	77.7 Wh/l	146 Wh/l
Operation and storage temperature	$-25\,°C$ to $65\,°C$	$-40\,°C$ to $50\,°C$

ES is needed for PV systems that are used for hydrogen production because of the intermittent and fluctuating nature of solar power and the need to keep the electrolyser in production or idle mode and avoid a total shutdown. In Australia, PV systems are exposed to various weather conditions, including extreme heat in the summer and cool temperatures in winter, which affects the performance of the PV panels and the efficiency of the hydrogen production process.

The use of ES in this system allows for the storage of excess solar energy that can be used during times of low solar irradiance or high demand for hydrogen. This helps to ensure a consistent and reliable supply of hydrogen, which is essential for industrial and transportation applications [15].

3.2. Li-ion Capacitor and Li-ion Battery Degradation

Laboratory testing on LiC cells was performed to study their degradation behavior in different operating and environmental conditions. The aging tests were conducted by continuously charging and discharging the LiCs with a 100% cycle depth, and various C-rates and temperatures, as presented in [12]. The results of the tests were used to develop an aging model for the LiC cells, which was then used to predict the capacity fade of the LiC storage over a period of time and in variable temperature and load conditions [16]. From [16] the cycling aging was measured, where the capacity fade of the LiC ($Cf_{Cycling\ LiC}$) was approximated using Equations (2) and (3). In (2) A is the degradation factor of the LiC as a function of current (I) and temperature (T). $Cf_{Cycling\ LiC}$ is a function of the cycle count during simulation (nc), I and T. nc as a function of time is counted during the simulation using (1), where $Q_{present}$ is the cell storage capacity. In Figure 3, the expected number of

full equivalent cycles (FECs) of the LiC before reaching the 20% capacity fade at various temperatures and currents is presented.

$$\text{nc(t)} = \frac{\int I}{2 \cdot Q_{present}} dt \tag{1}$$

$$A(I,T) = 0.0027 - 0.00036 \cdot I + 7.79 \cdot 10^{-6} \cdot I^2 + 4.3 \cdot 10^{-7} \cdot I \cdot T + 8.85 \cdot 10^{-7} \cdot T \tag{2}$$

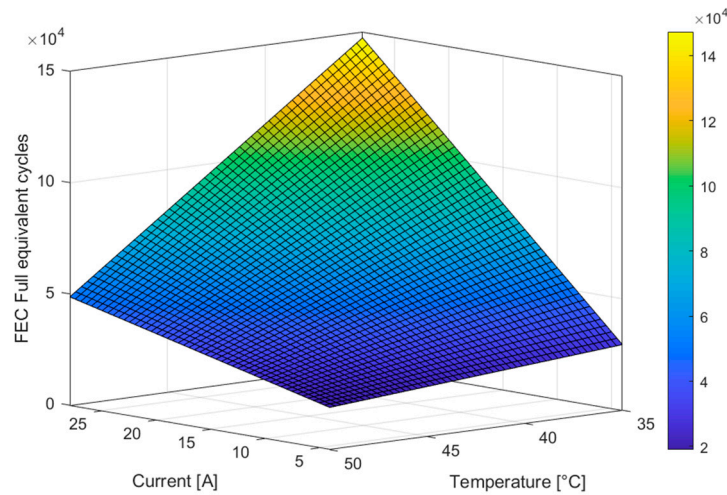$$Cf_{Cycling\ LiC}(t,I,T) = 100 - A(I,T) \cdot nc + A(I,T) \cdot nc^{0.95} \tag{3}$$

Figure 3. Full equivalent cycles (FEC) of LiC to drop to 80% of beginning-of-life capacity.

The data for the LiB degradation behavior analysis was obtained from the literature [17–19], and the cycling capacity fade is estimated using the model formulated in (4) and (5). $End\_of\_life\_FEC_{LiB}$ is the expected number of FECs that the LiB can withstand at various temperatures and currents before reaching the 20% capacity fade, which is presented in Figure 4.

$$End\_of\_life\_FEC_{LiB}(I,T) = 2.4 \cdot 10^4 + 573.1 \cdot I - 904 \cdot T - 9.6 \cdot I \cdot T + 9.1 \cdot T^2 \tag{4}$$

$$Cf_{Cycling\ LiB}(t,I,T) = \frac{20\% \cdot nc}{End\_of\_life\_FEC_{LiB}} \tag{5}$$
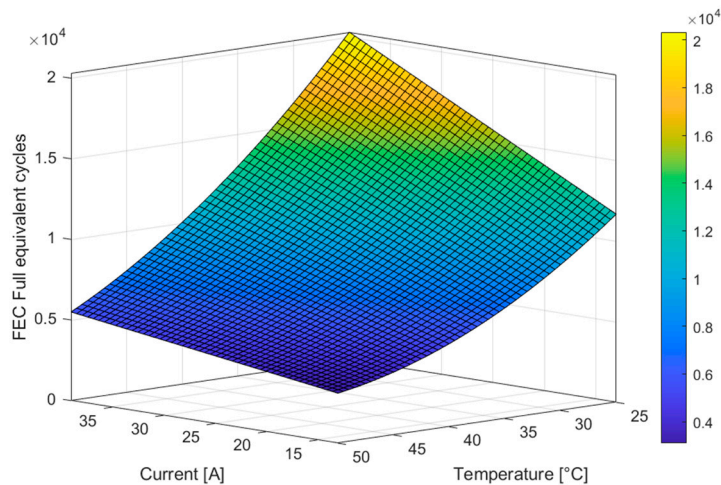

Figure 4. Full equivalent cycles (FEC) of LiB to drop to 80% of beginning-of-life capacity.

Overall, the laboratory testing and degradation behavior analysis demonstrated the superiority of LiC over LiB as an energy storage solution in applications that makes high FEC and are placed outdoors; however, by considering the calendar aging of LiC and LiB it is found that the calendar aging effect on the LiB is very small (0.8% capacity loss per year) [18] compared to the calendar aging of the LiC cells which is dependent on the idle time conditions of the LiC, such as SoC and the temperature, as shown in Figure 5. The capacity fade caused by calendar aging of the LiC $Cf_{calendar\_LiC}$ as a function of SoC and T is formulated in (6) and derived from the calendar aging test performed in [20] and aligned with the shelf life from the LiC datasheet (5 years shelf life at room temperature and 0% SoC). $Cf_{calendar\_LiC}$ is the percentage of the faded capacity over the time (t) before the end of life (EOL) which is a 20% loss of the starting capacity.

$$Cf_{calendar\_LiC}(SoC, T) = \frac{20\% \cdot \left(101.7 + 1.018 \cdot SoC - 0.57 \cdot T + 0.0053 \cdot SoC \cdot T - 0.01 \cdot T^2\right)}{t} \tag{6}$$
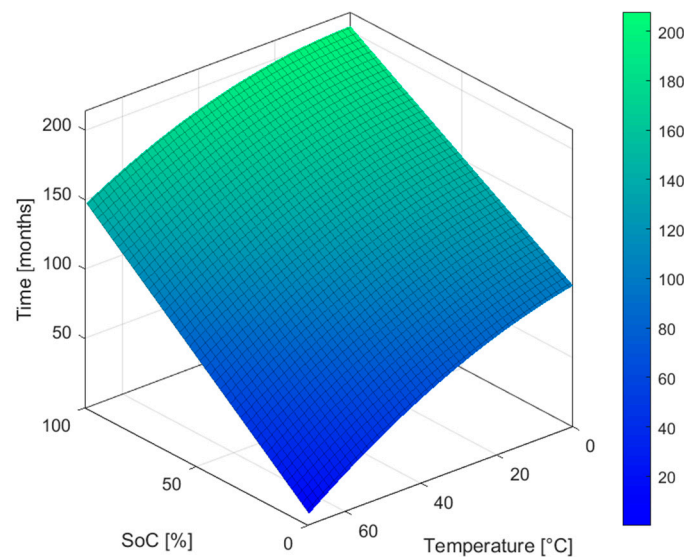

Figure 5. The expected calendar life, expressed in months of the LiC at various SOCs and temperatures, for an EOL criterion of a 20% capacity fade.

3.3. Li-ion Capacitor and Li-ion Battery Internal Resistance Development

The internal resistance (IR) development during the lifetime of the ES is an important parameter that governs the response behavior of the ES in regulating the grid. IR increase due to the aging of LiC and LiB is studied and modeled.

The [20] IR increase due to calendar aging is modeled in Figure 6 which presents the required time in months to have a 200% increase in the LiC IR. The LiC IR increase due to calendar aging was modeled as a function of temperature and SoC.

In [16] the LiC IR increase due to cycling aging ($IR_{CYCLING\_LiC}$) was approximated using Equations (7) and (8). In (7), B is the IR increasing factor of the LiC as a function of current (I) and temperature (T) and $ESR_{CYCLING\_LiC}$ is a function of the cycle count during simulation (nc), I and T.

$$B(I, T) = -0.0076 - 0.0013 \cdot I + 3.3 \cdot e^{-5} \cdot I^2 - 3.7 \cdot e^{-6} \cdot I \cdot T + 0.0008 \cdot T - 1.8 \cdot e^{-7} \cdot T^2 \tag{7}$$

$$IR_{CYCLING\_LiC}(t, C - rate, T) = 100 - B_{C-rate,T} \cdot nc + B_{C-rate,T} \cdot nc^{0.95} \tag{8}$$
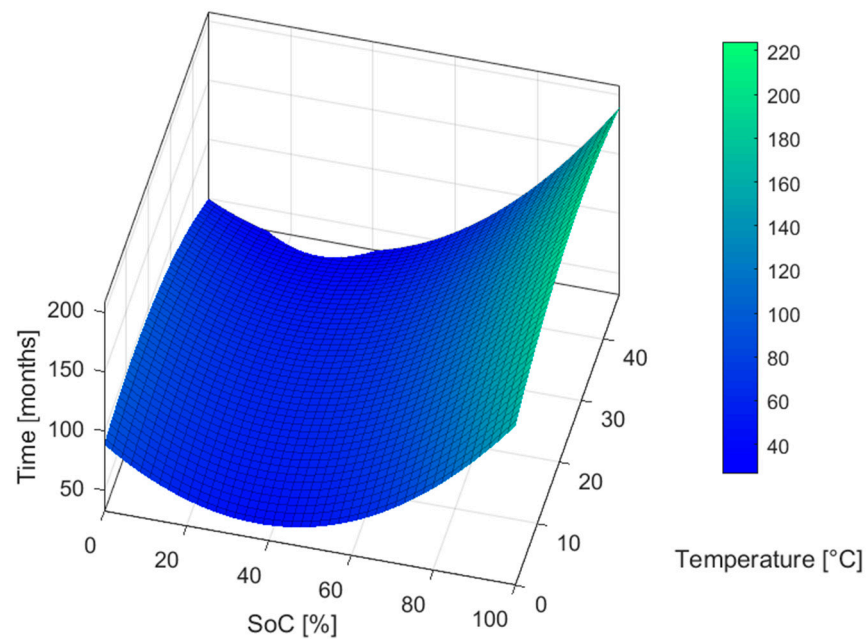
Figure 6. The expected time, expressed in months, for the LiC to increase the IR to 200% due to calendar aging.

From [18], the $IR_{CYCLING\_LiB}$ is approximated to increase by 10% for each 3000 FEC. The time required for the IR of the LiB to increase by 200% was modeled as a function of idling SOC and temperature and the results are presented in Figure 7.
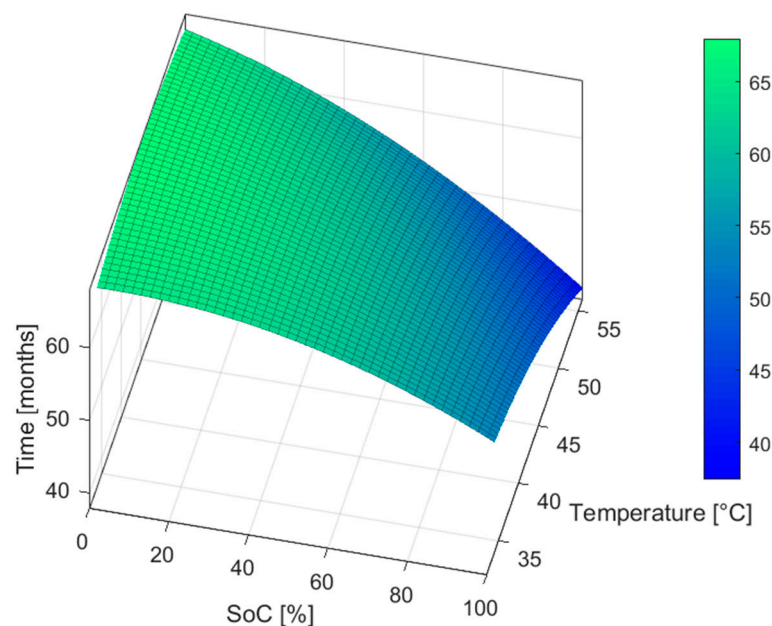
Figure 7. The expected time, expressed in months, for the LiB to increase the IR to 200% due to calendar aging.

It can be noticed that for the case of the IR, idling at lower SoCs for the LiBs has the opposite effect than for LiCs and elongates the calendar lifetime.

4. Storage System Sizing for the Australian Climate

In Figure 8, the simulation model for the considered system is presented showing the PV source, electrolyser load, EMS and ES. The system model is used for iterative

simulations for 10 years period (2012 to 2022) to be used for optimizing the system size. The components of the system are described as follows:

- PV source is a 1500 W nominal capacity. PV capacity size is fixed for all test cases.
- Electrolyser for hydrogen generation is 1000 W in generation mode and 100 W in idle mode (Two electrolyser units are used).
- EMS as described in Figure 2. The state machine governs the load operation and the states where the power from the PV is delivered to the load or the energy storage.
- Energy storage unit (ES) represents the LiC or the LiB models including the aging models of each energy storage technology.
- System model inputs are the temperature and irradiation for 10 years at Brisban, Australia. Output signals such as the SoC and ES capacity fade over 10 years [21]. Irradiation forecast is also considered as an input to the EMS state machine.
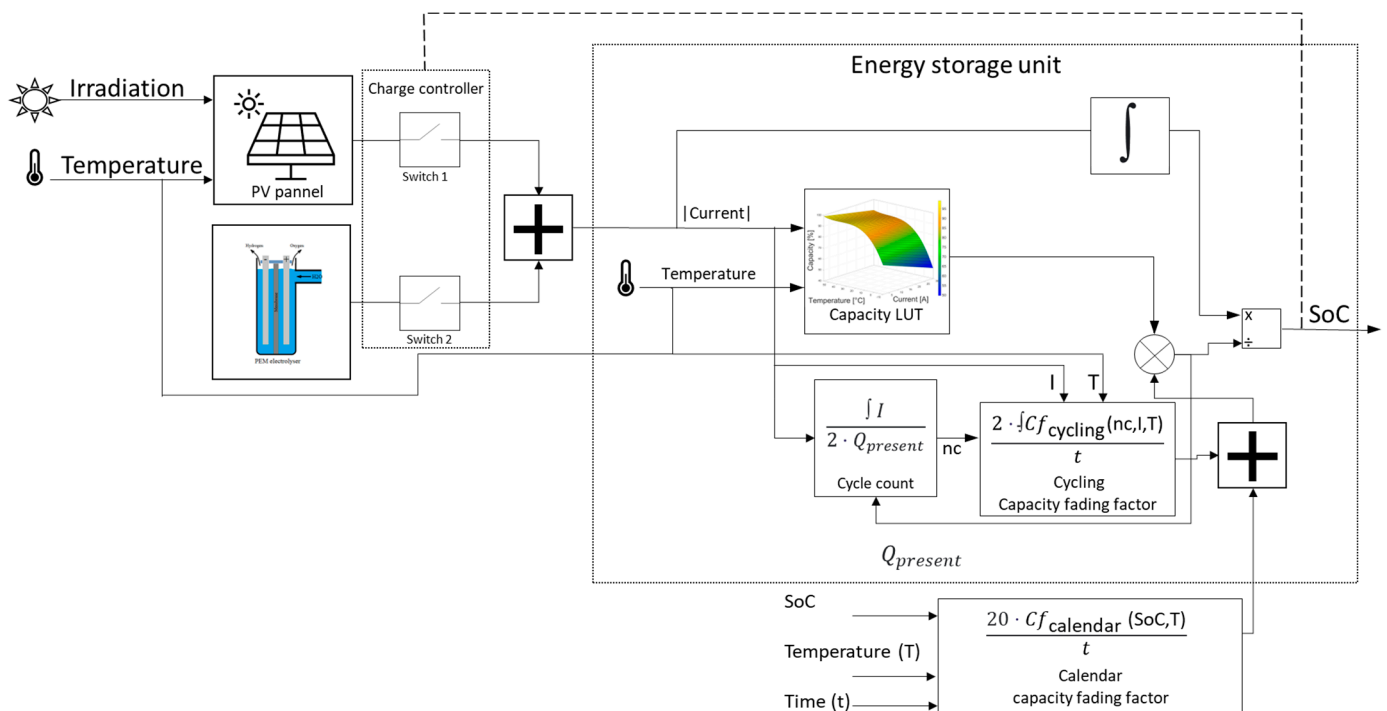

Figure 8. Green hydrogen production from the PV system model for simulation.

After setting the system model the sizing process starts.

In the literature, several optimization algorithms are used depending on the complexity and the number of optimized parameters. While the sparrow search algorithm can be used for a multi-dimensional problem such as day-ahead active power scheduling [8], hill climbing sizing problems only need a directed search algorithm that changes one parameter, simulate, evaluate and iterate [7]. The goal of the algorithm, which is presented in Figure 9, is to find the optimal ES size with a similar method to perturb and observe what increases or decreases the size in such a manner to speed up the sizing process.

The objective of the sizing is to have the optimal storage size that sustains the operation of the system during the night. The used constraint for sizing was fail mode avoidance where fail mode happens if the ES could not meet the demand of the electrolyser. The sizing process has two parts: the simulating modeled system in Figure 8 and the evaluation of the outputs through the algorithm in Figure 9.
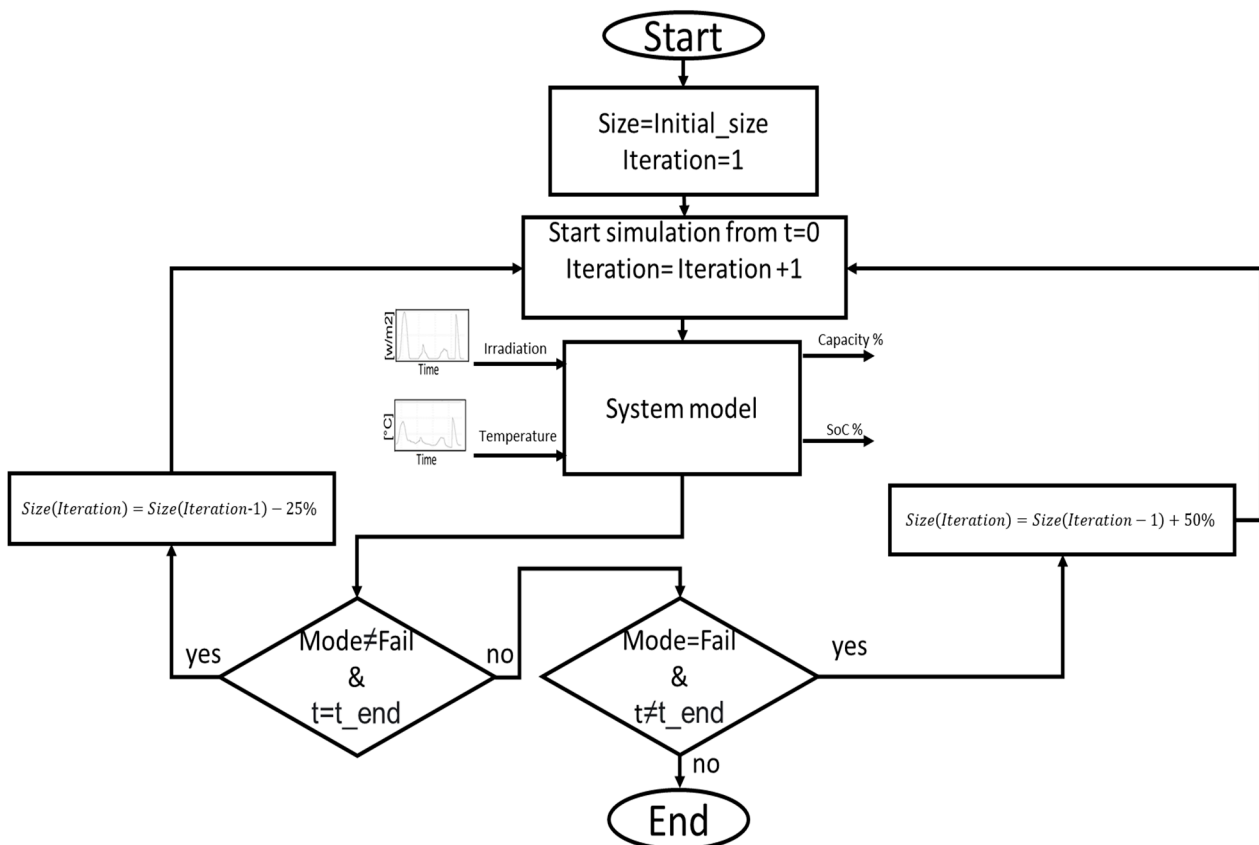
Figure 9. ES optimization algorithm using system simulation of green hydrogen production from PV.

The process starts by setting the initial size of the simulation and the iteration number and then running the simulation. If the output load signal does not show a fail state (Load = 0) and the simulation has reached the end time (t = t_end), the size of the simulation is reduced by 25% and the iteration number is incremented. The process then runs the simulation again from t = 0 with the new size. If the mode of the system is "Fail" and the simulation has not reached the end time (t ≠ t_end), the size of the simulation is increased by 50% and the iteration number is incremented and the simulation starts over. The sizing process ends when the system is not in the fail mode and the time reached t_end in the simulation.

In the next section, the system is sized for different cases and the results are analyzed.

5. Sizing Results for the Li-ion Capacitor and Li-ion Battery

In Table 2, six different sizing cases for both the LiC and LiB as ES for the green hydrogen system are presented. Each case has a different EMS state machine setting named idle,1, 2, and 3. Each EMS state machine number represents a different SoC threshold for the transition from production mode to idle mode as shown in Figure 2 to match the production time during the night with the ES size. Depending on the Irradiation forecast SoC threshold is selected, and whether the transition from production to idle mode happens at a high SoC (SoC_threshold1= 60 to 30%) and the night production is reduced or at low SoC (SoC_threshold2 = 25% in all cases) where the night production is increased. While the idle state machine secures the required power for the electrolyser to remain in idle mode during the night. The size is presented as the number of cells and Ah size. The size of the LiC is considered 100% for comparison purposes between LiC and LiB and illustrates the oversizing. The capacity fade is measured at the end of 10 years of operation where the fade is due to both cycling and calendar aging. For each case, the energy delivered to the electrolyser is represented in the parameter electrolyser load per year.

Table 2. Comparison between LiC and LiB ES for the green hydrogen production from PV (*refers to the remaining capacity after 10 years of operation).

Cases	LiC					LiB					State Machine for ES (SoC_threshold1)	Electrolyser Load per Year [MWh]
	LiC Size [Cells]	Size [Ah]	LiC Size [%]	Remaining Capacity * [%]	LiC IR [%]	LiB Size [cells]	Size [Ah]	LiB Size [%]	Remaining Capacity * [%]	LiB IR [%]		
1	1610	6440	100	80.8	260	620	8680	135	89.4	342	3	5.23
2	910	3640	100	80.60	262.6	368	5152	142	87.87	344.7	(SoC ≤ 30%)	4.83
3	710	2840	100	80.3	263.6	287	4018	141	87	346	2 (SoC ≤ 40%)	4.58
4	610	2440	100	80.2	264	247	3458	142	86.45	346.7	1	4.39
5	528	2112	100	79.8	265.6	214	2996	142	85.8	348	(SoC ≤ 50%)	4.24
6	280	1120	100	80.3	270	117	1638	146	83.3	353	Idle (SoC ≤ 60%)	3.2

As it can be seen from Table 2 and Figure 10, increasing the size of the ES is reflected in the delivered energy to the electrolyser which means higher production of hydrogen. However, the relation is exponential as shown in (9) and (10).

$$\text{Electrolyser\_load\_per\_year}_{LiC} = 4.8 \cdot e^{(1.326 \cdot 10^{-5} \cdot \text{size})} - 3.4 \cdot e^{(-0.00072 \cdot \text{size})} \tag{9}$$

$$\text{Electrolyser\_load\_per\_year}_{Lib} = 4.67 \cdot e^{(1.347 \cdot 10^{-5} \cdot \text{size})} - 3.6 \cdot e^{(-0.00057 \cdot \text{size})} \tag{10}$$
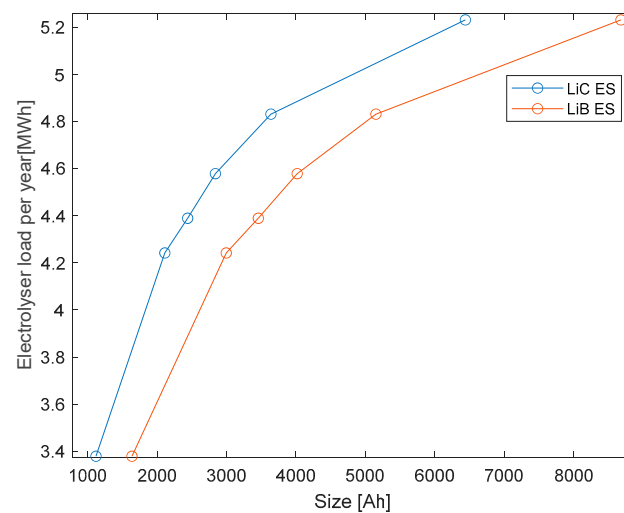
Figure 10. Sizing of LiC and LiB ES and the energy delivered to the electrolyser per year.

From Figure 10, it was found that LiB is oversized in all cases compared to LiC. In Figure 11, the green hydrogen production from the PV system was simulated for 14 days for cases 1, 3 and 6. Case 6 (blue) represents the smallest ES size where the storage only secures the power to the electrolyser to remain in the idle mode and avoid total shutdown, while Case 1 (red) represents the biggest ES size which powers the electrolyser load during the night to produce hydrogen. Case 1 also shows that the ES is not charged to 100% SoC during the day because it takes a longer time to be fully charged (PV capacity is fixed for all cases while the ES size increases) and this causes a higher effect of calendar aging in the case of LiC ES. The LOAD (H2 Electrolyser) shows that the electrolyser works with full capacity during the day in Case 6 because the ES is small in this case to deliver 10% of the

load power during the night while in Case 1 the ES is large enough to keep the electroryser during the night. The results in Figure 11 are from LiB ES simulation but it applies for both LiC and LiB in terms of the delivered power to the load as they are sized in each case to provide the same power.
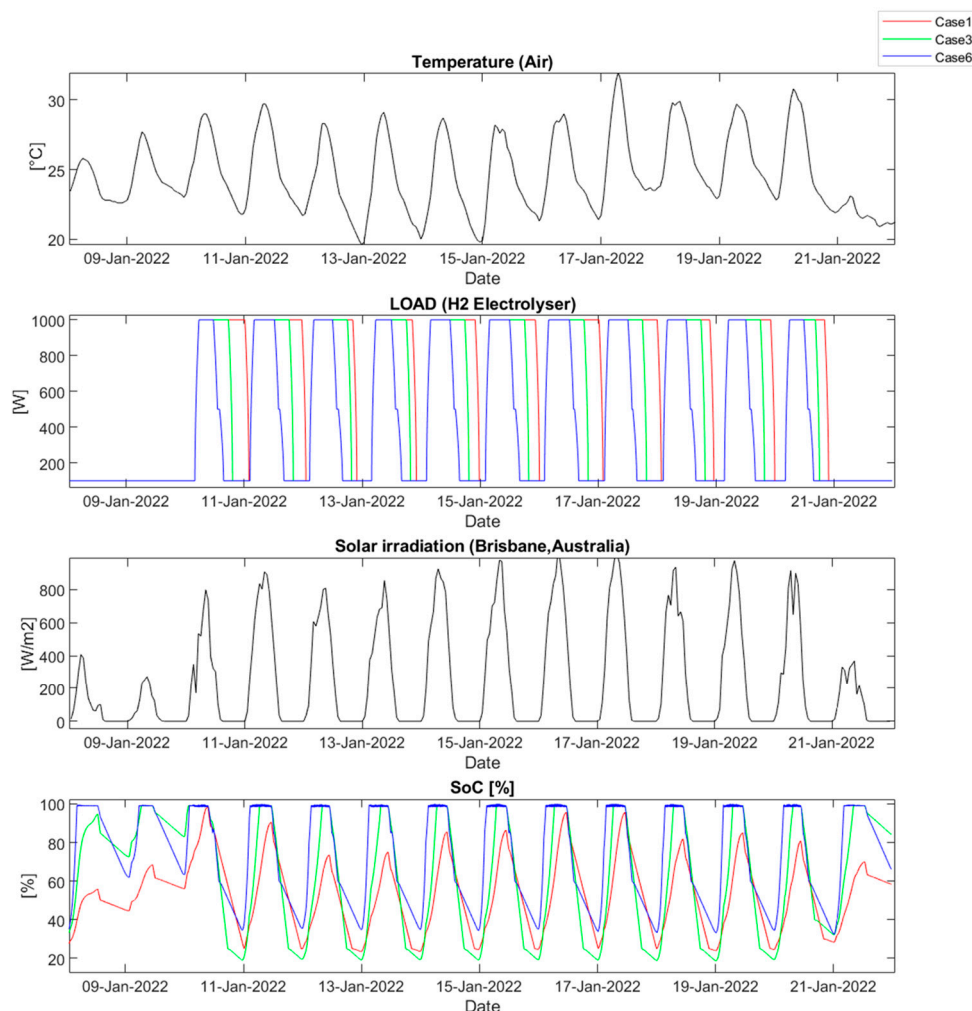

Figure 11. Simulation of 14 days of the system showing the temperature, irradiation, electrolyser load and SoC for cases 1,3 and 6. These results are from LiB ES simulation.

In Figure 12, the histogram plots show that the ES spends more time in low SoC in big ES such as Case 1 and spends more time in higher SoC in small ES such as Case 6, and from Figure 5, it is known that lower SoC for longer time shortens the calendar life of the ES; however, smaller ES sizes have a higher cycling aging compared to the bigger ES scenarios. Figure 13 represents the relation between the electrolyser energy in MWh and the capacity fading percentage. Increasing the energy storage size leads to increased electrolyzer load energy, and decreased aging due to cycling, but it also increases the aging due to staying in a low state of charge (SoC) for longer periods. This impact is more visible in the LiC energy storage system. LiB has longer retention of capacity but comes with an increased IR to around 350% after 10 years of operation, while LiC has a less IR increase to around 265% in the same period as shown in Figure 14.
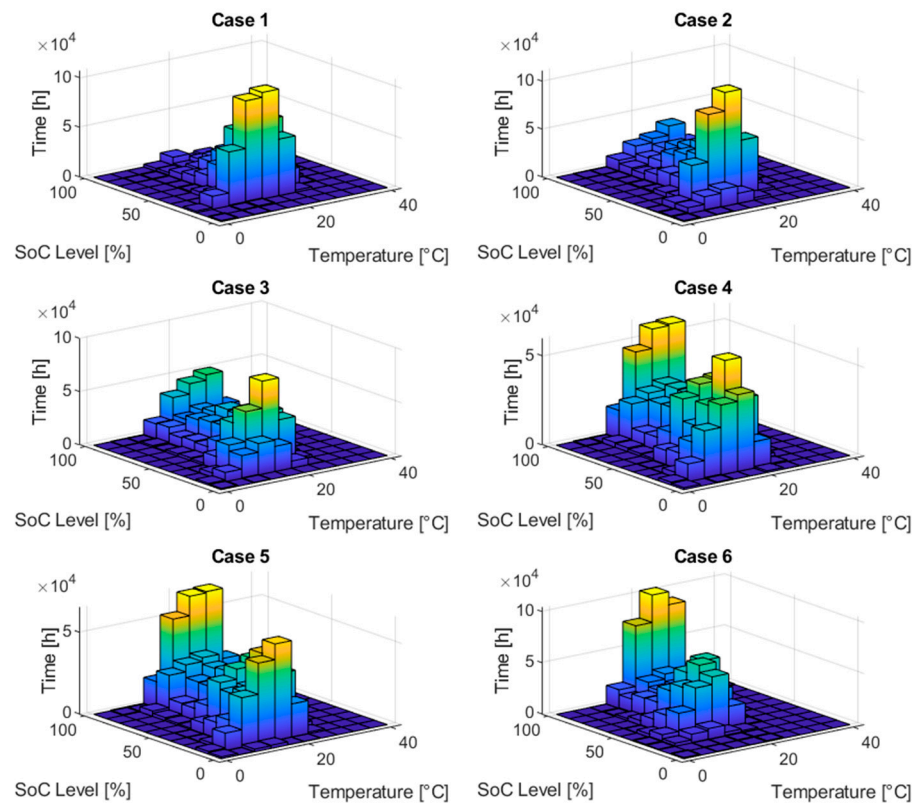
Figure 12. 3D histogram of the simulated 6 cases showing the time ES spent on each temperature and SoC state.
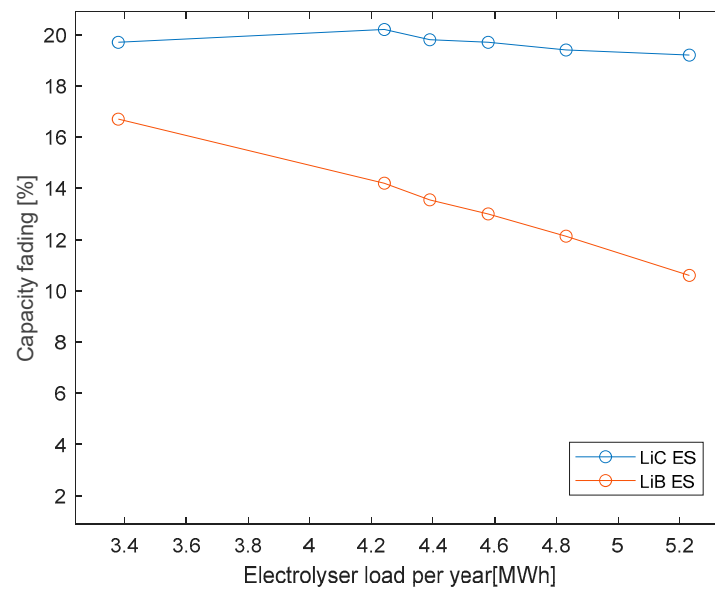

Figure 13. Capacity fade of the LiC and LiB ES as a function of the energy delivered to the electrolyser load.
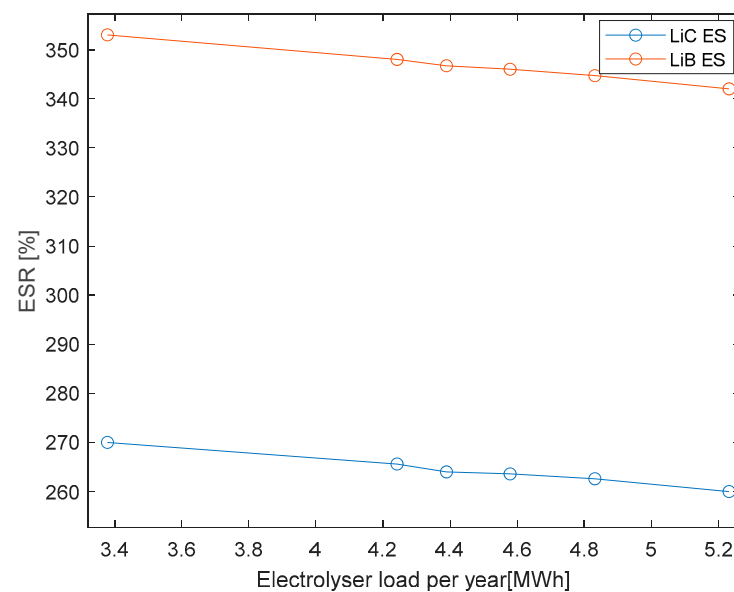
Figure 14. IR of the LiC and LiB ES after 10 years of operation as a function of the energy delivered to the electrolyser load.

Maintaining low IR is important when using ES not only for energy storage but also for grid regulation, where the ES is used to provide a rapid response by either absorbing or injecting power into the grid. High IR is also a sign of lower efficiency of the ES and increasing power losses [14].

In Table 2, while each case was sized using the algorithm in Figure 9 to achieve the same Energy Delivered to Electrolyser for LiC and LiB, it was found that LiB is oversized in all cases compared to LiC. However, LiC has a smaller remaining capacity compared to LiB after 10 years of operation which makes the LiB a better ES for the application, but considering the IR and the need to use the ES for grid regulation, LiC is the better option because lower IR means better response to the grid which suffers from the power fluctuations from PV. From Figure 12 it is found that case 4 has an even distribution of high and low SoC stay time, where the effect of calendar aging and cycling aging is minor in the case of LiC. LiB performs better in cases 5 and 6 because LiB is not affected much by the calendar capacity fade, and upsizing the ES in the case of LiB means a higher energy production for green hydrogen and a lower capacity fade by 6%. LiC has a high potential in the green hydrogen production from PV if the low IR is required in the grid design for better response and lower power losses due to ES degradation.

6. Discussion and Future Work

The motivation behind this work was driven by the increasing trend of green transitioning initiatives undertaken by governments worldwide. One such project is the Redlands Research Facility located east of Brisbane, Australia, which aims to establish a green hydrogen plant using locally produced solar energy. The green hydrogen pilot plant consists of a microgrid that uses concentrated-PV (CPV) and PV arrays, backed with commercially available batteries, to enhance its energy efficiency and a 40 kW PEM electrolyser [5] supplied with 5.5 L per hour of water. The project aimed to provide experimental validation and an integrated modeling of a hybrid renewable energy process that utilizes solar power, energy storage, and non-potable water to produce, store, and use hydrogen.

Another approach that arised within the project was to develop a fully DC microgrid that eliminates the unnecessary AC conversion components from the hydrogen production microgrid [12]. This led to the development of a downscaled fully DC hydrogen generation microgrid and a 500 W electrolyser and energy storage were required [9].

Using LiC was proposed for this application as an alternative energy storage to LiB, because of LiC's promising characteristics and the advantages provided by the hybridization of supercapacitors and Li-ion batteries [4].

Commercially available LiC cells were tested for characterization under different conditions and went through an extensive aging test, where each cell went under different aging conditions to model its performance and aging behavior and predict its performance in different climates using system simulation [16].

The aging models for both LiC and LiB were derived from lab tests and the literature. An EMS was modeled to imitate the operation of the green hydrogen microgrid, and the system was modeled and used to make a size optimization and estimation of the degradation happening to the energy storage after an operation of 10 years. The results show that LiC has a lower optimal size in terms of Ah compared to LiB because of its temperature tolerance and it degrades much slower in terms of FEC; however, LiC loses much of its capacity due to calendar aging which is not very effective on the LiB. Though, calendar aging increases the internal resistance of the LiB more than the LiC.

Future work will consider the usage of LiC for grid regulation and power smoothing as well as using it for storage. Also, it will consider the power generation data from the CPV and PV at the Redlands facility and make a comparison between the performance of the LiC regulating the grid at the beginning and after years of operation where the performance is dependent on the remaining capacity and the internal resistance.

7. Conclusions

The study provides an analysis of Li-ion capacitors and Li-ion batteries as energy storage systems for green hydrogen production from PV in the Australian climate. The study compares the performance of LiC and LiB in six different cases using four modes of EMS state machines and a sizing algorithm that optimize the energy storage to secure a safe operation of the electrolyser and increase its productivity. The EMS state machine has an idle mode where the size is minimum and the ES is required only to deliver 10% of the electrolyzer load power to avoid a total shutdown. The other EMS modes are operating the system for different sizes. The EMS uses inputs such as irradiation and irradiation forecast and temperature from the plant location. The system model is used for iterative simulations for 10 years period to be used for optimizing the system size. A directed search algorithm was used to reduce the number of search iterations in the sizing process. The results show that LiB is oversized in all cases compared to LiC, but LiC has a smaller remaining capacity after 10 years of operation due to the higher calendar aging. However, considering the IR and the need to use energy storage for grid regulation, LiC can be a better option because a lower IR means a better response to the grid. Additionally, IR after 10 years of operation for LiC is 264% of its initial IR, while for LiB it is 346%. Furthermore, the average remaining capacity after 10 years of operation for LiC is 80.2%, while for LiB it is 86%. These results indicate that while LiB may have a higher remaining capacity, it also has a higher IR. The study shows that Li-ion battery performs better in cases not affected much by the calendar capacity fade and upsizing the energy storage in the case of Li-ion battery means a higher energy production for green hydrogen and a lower capacity fade by 6%. Overall, LiC has a high potential in green hydrogen production from PV if the low IR is required in the grid design for better response and lower power losses due to energy storage degradation.

Author Contributions: Methodology, T.I. and S.S.M.; Investigation, T.I. and D.S.; Resources, T.K., D.S. and D.-I.S.; Writing – original draft, T.I.; Writing – review & editing, T.I., T.K. and D.-I.S.; Supervision, T.K., D.S. and D.-I.S. All authors have read and agreed to the published version of the manuscript.

Nomenclature

Notation	Definition	Unit
LiC	Li-ion Capacitor	-
LiB	Li-ion Battery	-
Cf	Capacity Fade	-
nc(t)	Cycle count during simulation	-
IR	Internal Resistance	Ω
SoC	State of Charge	%
ES	Energy Storage	-
PV	Photovoltaic	-
CPV	Concentrated Photovoltaic	
EMS	Energy Management System	-
MWh	Megawatt-hours	-
EOL	End of Life	-
T	Temperature	$^{\circ}$C
I	Current	A
t	Time	s
t_end	End time of simulation	-
Q_present	Cell storage capacity	Ah
SoC_threshold1	State of Charge threshold for transition from Production to Idle mode	%
SoC_threshold2	State of Charge threshold to remain in production mode	%
fail	Fail state of the electrolyser (total shut down)	-
idle	idle state of the electrolyser (10% of the rated power)	-

References

1. Huang, F.; Liu, J.; Wang, Z.; Shuai, C.; Li, W. Of jobs, skills, and values: Exploring rural household energy use and solar photovoltaics in poverty alleviation areas in China. *Energy Res. Soc. Sci.* **2020**, *67*, 101517. [CrossRef]
2. Jung, W.; Jeong, J.; Kim, J.; Chang, D. Optimization of hybrid off-grid system consisting of renewables and Li-ion batteries. *J. Power Sources* **2020**, *451*, 227754. [CrossRef]
3. Thampan, T.; Ding, Y.; Toomey, L.; Hundich, A.; Babu, V. Accelerated Degradation of Li-Ion Batteries for High Rate Discharge Applications. In Proceedings of the Ground Vehicle Systems Engineering and Technology Symposium, Novi, Michigan, 11–13 August 2020; pp. 13–15.
4. Ibrahim, T.; Stroe, D.; Kerekes, T.; Sera, D.; Spataru, S. An Overview of Supercapacitors for Integrated PV—Energy Storage Panels. In Proceedings of the 2021 IEEE 19th International Power Electronics and Motion Control Conference (PEMC), Gliwice, Poland, 25–29 April 2021; pp. 828–835.
5. Mohammadshahi, S.S.; Boulaire, F.A.; Love, J.; Gorji, S.A.; Mackinnon, I.D. A flexible analytical model for operational investigation of solar hydrogen plants. *Int. J. Hydrog. Energy* **2022**, *47*, 782–808. [CrossRef]
6. Hernández, J.C.; Sanchez-Sutil, F.; Muñoz-Rodríguez, F.J. Design criteria for the optimal sizing of a hybrid energy storage system in PV household-prosumers to maximize self-consumption and self-sufficiency. *Energy* **2019**, *186*, 115827. [CrossRef]
7. Hernández, J.C.; Gomez-Gonzalez, M.; Sanchez-Sutil, F.; Jurado, F. Optimization of battery/supercapacitor-based photovoltaic household-prosumers providing self-consumption and frequency containment reserve as influenced by temporal data granularity. *J. Energy Storage* **2021**, *36*, 102366. [CrossRef]
8. Wenzhi, S.; Zhang, H.; Tseng, M.L.; Weipeng, Z.; Xinyang, L. Hierarchical energy optimization management of active distribution network with multi-microgrid system. *J. Ind. Prod. Eng.* **2022**, *39*, 210–229. [CrossRef]
9. Ganjavi, A.; Gorji, S.; Hakemi, A.; Moradi, A.; Sera, D. Design and Implementation of an SiC-Based 48 V-380 V Dual Active Bridge DC-DC Converter for Batteries Employed in Green Hydrogen Microgrids. In Proceedings of the 7th IEEE Southern Power Electronics Conference (SPEC 2022), Denarau Island, Fiji, 5–8 December 2022.
10. Schmidt, O.; Gambhir, A.; Staffell, I.; Hawkes, A.; Nelson, J.; Few, S. Future cost and performance of water electrolysis: An expert elicitation study. *Int. J. Hydrog. Energy* **2017**, *42*, 30470–30492. [CrossRef]
11. Carmo, M.; Fritz, D.L.; Mergel, J.; Stolten, D. A comprehensive review on PEM water electrolysis. *Int. J. Hydrog. Energy* **2013**, *38*, 4901–4934. [CrossRef]
12. Gorji, S.; Sera, D. Projects: Fully DC Microgrid for Green Hydrogen Production. QUT Centre for Clean Energy Technologies and Practices. Available online: research.qut.edu.au/ccetp/projects/fully-dc-microgrid-for-green-hydrogen-production (accessed on 20 October 2022).
13. Matute, G.; Yusta, J.M.; Beyza, J.; Correas, L.C. Multi-state techno-economic model for optimal dispatch of grid connected hydrogen electrolysis systems operating under dynamic conditions. *Int. J. Hydrog. Energy* **2021**, *46*, 1449–1460. [CrossRef]

14. Soltani, M.; Ibrahim, T.; Stroe, A.I.; Stroe, D.I. Comparison of High-Power Energy Storage Devices for Frequency Regulation Application (Performance, Cost, Size, and Lifetime). In Proceedings of the IECON 2022–48th Annual Conference of the IEEE Industrial Electronics Society, Brussels, Belgium, 17–20 October 2022; pp. 1–6.
15. Cerniauskas, S.; Grube, T.; Praktiknjo, A.; Stolten, D.; Robinius, M. Future hydrogen markets for transportation and industry: The impact of CO_2 taxes. *Energies* **2019**, *12*, 4707. [CrossRef]
16. Ibrahim, T.; Kerekes, T.; Sera, D.; Stroe, D.I. Degradation Behavior Analysis of High Energy Hybrid LITHIUM-Ion Capacitors in Stand-Alone PV Applications. In Proceedings of the IECON 2022–48th Annual Conference of the IEEE Industrial Electronics Society, Brussels, Belgium, 17–20 October 2022; pp. 1–6.
17. Stroe, A.I.; Knap, V.; Stroe, D.I. Comparison of lithium-ion battery performance at beginning-of-life and end-of-life. *Microelectron. Reliab.* **2018**, *88*, 1251–1255. [CrossRef]
18. Stroe, A.I. *Analysis of Performance and Degradation for Lithium Titanate Oxide Batteries*; Aalborg University Press: Aalborg, Denmark, 2018.
19. Stroe, A.I.; Stroe, D.L.; Knap, V.; Swierczynski, M.; Teodorescu, R. Accelerated Lifetime Testing of High Power Lithium Titanate Oxide Batteries. In Proceedings of the 2018 IEEE Energy Conversion Congress and Exposition (ECCE), Portland, OR, USA, 23–27 September 2018; pp. 3857–3863.
20. Soltani, M.; Ronsmans, J.; Van Mierlo, J. Cycle life and calendar life model for lithium-ion capacitor technology in a wide temperature range. *J. Energy Storage* **2020**, *31*, 101659. [CrossRef]
21. Solcast. Solar Irradiance and temperature Data, 2012–2022 Brisbane, Australia. Available online: https://solcast.com (accessed on 21 September 2022).